DEVELOPMENTAL BIOLOGY 174, 431–447 (1996)
ARTICLE NO. 0086

of the Sodium Pump Cloned from the Neural Plate of *Xenopus laevis*

C. S. Davies,[1] N. J. Messenger, R. Craig,[2] and A. E. Warner

Department of Anatomy and Developmental Biology, University College London, Gower Street, London WC1E 6BT

Expression of a catalytic α subunit of the sodium pump was followed in early *Xenopus* embryos for correlation with physiological experiments showing that the sodium pump controls cavity expansion and the differentiation of neurones from the neural plate. Two cDNAs (one full length, one partial) for α_1 subunit isoforms were cloned from a neural plate stage *Xenopus* library and sequenced. Other isoforms were not detected. Temporal and spatial expression patterns for α_1 subunit transcripts and protein revealed extensive developmental regulation. At all stages, cells involved in cavity generation (outer ectoderm and cells lining the archenteron) expressed α_1 transcripts with protein confined to the lateral and basal membranes. Before gastrulation, transcript levels were low and predominantly in animal cells. During gastrulation, α_1 mRNAs rose significantly. Transcripts and protein were down-regulated in future outer neural plate cells as the mesoderm invaginated. Protein appeared at the blastopore on apical surfaces of lip cells and apposing surfaces of invaginating cells, suggesting that the Na pump opposes entry of fluid. In early neurulae, α_1 mRNAs rose sharply. Transcript expression remained low in outer neural plate cells and increased in the endoderm, and protein appeared in the notochord. In midneurulae, transcripts returned in outer neural plate cells. Protein expression appeared on basal surfaces of deep neural plate cells and the floor plate, matching physiological observations. After neural tube closure, transcripts were detected in all dorsal structures. Protein was retained in the notochord and floor plate, was eliminated from the outer layer of the neural tube, and appeared on ependymal cells. The results are discussed in relation to previous physiological observations.

INTRODUCTION

The sodium–potassium-activated ATPase (the sodium pump) catalyzes the translocation of sodium and potassium across cell membranes. It is found in all animal cells and ensures that ionic and osmotic balance is maintained across the surface membrane. The sodium gradient fuels a number of transport systems and drives the bulk transport of salt across epithelia. During early development the sodium pump is involved not only in maintaining cellular ionic balance, but also in the formation of embryonic cavities, such as the blastocoel (amphibian, Slack *et al.*, 1973; Slack and Warner, 1973; mammalian, Biggers *et al.*, 1977). An important functional role for the sodium pump during neural development has been revealed in the amphibian embryo, where activation of additional sodium pumps in neural plate cells during the midneural fold stages generates a large electrogenic potential that adds to the resting potential (Blackshaw and Warner, 1976b) and reduces intracellular sodium in the neural plate (Breckenridge and Warner, 1982). These sodium pump driven changes in the physiological properties of neural plate cells are essential for the subsequent normal development of the nervous system. The consequences of preventing activation of the sodium pump during neurulation are catastrophic: primary neurones fail to differentiate from the neural plate and the cellular organiza-

Sequence data from this article have been deposited with the EMBL/GenBank Data Libraries. The accession numbers are pXen9, U49238; 2Ousb, U49239.

[1] Present address: The Wellcome Trust, 183 Euston Road, London NW1.

[2] Present address: Institute of Molecular Medicine, ICRF, John Radcliffe Hospital, Headington, Oxford OX3 9DU.

0012-1606/96 $18.00

tion of the developing brain and neural retina is destroyed (Messenger and Warner, 1979). The interval over which neuronal differentiation is sensitive to inhibition of the sodium pump is restricted to the midneural fold stages when the membrane potential is increasing. Blocking the sodium pump either earlier or later in neurulation has no effect on the differentiation of neurones (Messenger and Warner, 1979).

How are these alterations in sodium pump activity brought about? Blackshaw and Warner (1976b) showed that additional sodium pumps are inserted into the membranes of neural plate cells about 2 hr before the membrane potential begins to rise spontaneously, and one possibility is that endogenous activators switch on the pump. Growth factors and neurotransmitters, particularly monoamines, activate the sodium pump (Phillis and Wu, 1981) and monoamines such as noradrenaline and its synthetic precursors are present in the embryo at the appropriate stages (Rowe *et al.*, 1993). However, current evidence makes it unlikely that the pump is switched on by these monoamines (Rowe *et al.*, 1993). An alternative approach is to examine the regulation of expression of sodium pump genes during early development. The sodium pump is constructed from three subunits: α, β, and γ. The α subunit contains the catalytic element of the enzyme, while the β subunit is essential for the insertion of the α subunit into the membrane to form a functional enzyme and may play a role in membrane targeting and potassium sensitivity (see Chow and Forte, 1995, for review). The function of the γ subunit is still somewhat obscure. We have isolated cDNAs for an α_1 subunit of the sodium pump enzyme from the neural plate stage *Xenopus* embryo. The developmental regulation of the sodium pump in the *Xenopus* embryo has been explored through the spatial and temporal pattern of sodium pump α_1 subunit transcript expression together with an analysis of the spatial distribution of membrane-bound α_1 subunit protein between the 2-cell and swimming tadpole stages. The relationship between these expression patterns and previous physiological observations is discussed.

MATERIALS AND METHODS

Animals. Adult *Xenopus laevis* were induced to mate and lay eggs by injection of chorionic gonadotrophins into the dorsal lymph sac (600 IU for females; 400 IU for males). Alternatively, gonadotrophin-injected females were squeezed and the eggs fertilized artificially with a fresh suspension of testis macerated in 1/10 Ringer solution. Embryos were maintained in tap water or a dilute salt solution (m*M:* 11.9 NaCl, 0.14 $CaCl_2$, 0.14 KCl, 0.02 Ca $(NO_3)_2$, 0.065 $MgSO_4$, 0.23 Tris–HCl, 0.36 $NaHCO_3$, pH 7.4) until they reached the required stage. Embryos were staged according to the normal life table of *Xenopus laevis* (Nieuwkoop and Faber, 1967).

Isolation and analysis of cDNAs. A *Xenopus* stage 17 cDNA library (Kintner and Melton, 1987; generously provided by C. Kintner) was screened with a full-length cDNA for the sheep α_1 subunit of the sodium pump (Shull *et al.*, 1985; kindly donated by J. Lingrel). Positive clones were screened with fragments from the 5′ and 3′ ends of the sheep cDNA open reading frame and six clones that bound both 5′ and 3′ end fragments were taken for further analysis. All six clones gave identical restriction maps and had an identical sequence at the 5′ end, suggesting that they all represented copies of the same cDNA. The cDNAs were cloned into PTZ19 and one clone, pXen9, was chosen for full sequencing. Nested deletion clones were produced according to the method described in Ausubel *et al.* (1994). Both upper and lower strands were sequenced completely with the chain termination method (Sanger *et al.*, 1977) using a Sequenase kit (Amersham). Full-length pXen9 and fragments from the 5′ end, the midregion, and the 3′ end of the cDNA were cloned into Bluescript.

Analysis of RNAs. Embryos of the required developmental stages were homogenized in buffer (50 m*M* Tris–HCl, pH 7.5, 1 m*M* EDTA, 1% SDS, 0.3 *M* NaCl) and extracted twice in phenol/chloroform at room temperature, followed by ethanol precipitation at −20°C to extract total RNAs. Poly(A)$^+$ RNAs were isolated using a Qiagen kit from 700- to 900-μg samples of total RNA for each stage. Total RNA samples were dissolved in 500 μl DEPC distilled water. Five hundred microliters of 2× binding buffer (20 m*M* Tris–HCl, 1 *M* NaCl, 2 m*M* EDTA, 0.2% SDS, pH 7.5) and 55 μl Oligotex(dT) suspension (10% Oligotex in 10 m*M* Tris–HCl, 500 m*M* NaCl, 1 m*M* EDTA, 0.1% SDS, 0.1% NaN_3, pH 7.5), which had been warmed to 37°C, was added to each sample. After gentle mixing, tubes were incubated at 65°C for 3 min and hybridized at room temperature for 10 min. Tubes were then spun at 13,000 rpm for 2 min, supernatants were removed, and Oligotex(dT) pellets were resuspended in 400 μl wash buffer (10 m*M* Tris–HCl, 150 m*M* NaCl, 1 m*M* EDTA, pH 7.5) and transferred to spin columns. The columns were spun at 13,000 rpm for 30 sec, transferred to fresh tubes, and spun through a further 400-μl wash buffer. Columns were transferred to fresh tubes, 50 μl elution buffer (5 m*M* Tris–HCl, pH 7.5) at 70°C was added and mixed with the Oligotex(dT), and the tubes were spun again. After a final spin with the eluate, poly(A)$^+$ RNA was precipitated from the eluates in ethanol and stored at −80°C until used. For Northern analysis, either total RNA or poly(A)$^+$ RNA derived from the different developmental stages was separated by electrophoresis in denaturing formaldehyde–agarose gels. RNA was transferred to nylon membranes (Gene Screen Plus, Du Pont/NEN). Filters were hybridized with full-length gel-purified pXen9 cDNA labeled by random-primed synthesis and washed according to standard procedures (Sambrook *et al.*, 1989).

RNase protection assays were carried out as described by Melton *et al.* (1984). Briefly, probes were transcribed at 37°C for 60 min and template was removed with RNase-free DNase. A 200-nt antisense probe (20us6; bases 321–521 of pXen9) was used to detect α subunit RNAs. Ornithine decarboxylase levels, which change relatively little over the early developmental stages of *Xenopus* (see Isaacs *et al.*, 1992; L. Dale, personal communication and personal observations), were used to compare RNA loading in each lane and were detected with an ornithine decarboxylase probe (ODC; Isaacs *et al.*, 1992; obtained from Dr. L. Dale). Probes were gel purified and coprecipitated with RNA extracted from five embryos for each stage (5 to 10 μg RNA). The pellets were resuspended in 40 μl hybridization salts (40 m*M* Pipes, pH 6.4, 1 m*M* EDTA, pH 8.0, 0.4 *M* NaCl) with 80% formamide, denatured, hybridized overnight, and digested with RNase T1. Protein was removed with 50 μg proteinase K in 0.5% SDS. Samples were then phenol/chloroform extracted, reprecipitated in ethanol at −20°C, pelleted, resuspended in buffer, denatured at 80°C for 5 min, and run on a sequencing gel. Autoradiographs were scanned with a Bio-Rad scanning densitometer and the intensity of the pXen9 and ODC signals was mea-

sured using Molecular Analyst software (Bio-Rad). The pXen9 signal was expressed relative to that for ODC and plotted against time after fertilization and developmental stage.

In situ hybridization. Whole-mount *in situ* hybridization was carried out on normal *Xenopus* embryos according to the method of Harland (1991). Briefly, embryos were incubated in 10 μg/ml proteinase K (Sigma) at room temperature for 5–20 min (depending on the titer of the enzyme), prehybridized for 6 hr at 60°C in buffer (50% formamide, 5× SSC, 500 μg/ml torula RNA, 100 μg/ml heparin, 1× Denhardt's (Sigma), 0.1% Tween 20 (Sigma), 0.1% Chaps (3[(3-cholamidopropyl)-dimethylammonio]-1-propane sulfonate), 5 m*M* EDTA (ethylene diamine tetraacetic acid)) and then hybridized overnight with 500 μg/ml probe in the same buffer. The embryos were washed several times, incubated for 30 min in 20 μg/ml RNase (Sigma and Gibco-BRL) at 37°C to remove nonspecific RNAs, and washed again. Embryos were blocked with 20% heat-treated sheep serum for 1 hr, then incubated overnight in 1:2000 affinity-purified sheep anti-digoxigenin coupled to alkaline phosphatase (Boehringer). Sheep serum was not included in the antibody incubation as background was not significantly reduced by its presence. Embryos were incubated overnight in an NBT (Nitro Blue tetrazolium)/BCIP (5-bromo-4-chloro-3-indolyl phosphate) solution (Boehringer) to reveal staining and fixed in MEMFA (0.1 *M* Mops, pH 7.4, 2 m*M* EGTA, 1 m*M* $MgSO_4$, 3.7% formaldehyde) to stabilize the stain. Stained embryos were dehydrated in a graded series of alcohols and infiltrated (83% hydroxyethyl methacrylate, 17% butoxyethanol, 0.1% benzoyl peroxide) for 2 to 3 hr at room temperature. They were embedded in methacrylate at room temperature overnight, attached to chucks, and sectioned at 7 μm on a Sorvall JB-4 microtome. When necessary the embryos were oriented into the required plane and reembedded before sectioning. Transcripts were detected with anti-sense RNA probes transcribed from either the full-length pXen9 cDNA cut from Bluescript with *Hin*dIII or a 200-nt probe (20us6; bases 321–521). Both probes gave identical distribution patterns. Sense probes were used as controls and gave negligible stain. All probes were purified using nuc trap push columns (Stratagene) and stored in hybridization buffer at −20°C until used. Methacrylate sections gave excellent preservation of the hybridization signal along with good histology. Hybridization directly to frozen sections of unfixed embryos was both difficult and time consuming because of the fragility of embryos at early stages of development and was used only to confirm patterns of expression observed with the whole-mount schedule.

Sodium pump antibodies. Two affinity-purified anti-peptide antibodies, NASE (asparagine-alanine-serine-glutamic acid) and NPSE (asparagine-proline-serine-glutamic acid), raised against α_1 subunit-specific peptides, were used for the localization of the sodium pump. Affinity-purified NASE antibodies were kindly donated by Professor T. Pressley and have already been fully described (Pressley, 1992). They identify those vertebrate α_1 subunits that possess the NXSE amino acid motif and recognize a single band of about 100 kDa in Western blots (see Pressley, 1992). A band of almost identical size to that found in extracts of rat brain was recognized by NASE antibodies in extracts of *Xenopus* kidney and embryos. A second set of polyclonal antibodies (NPSE) were raised in rabbits against a 13 amino acid peptide drawn from the equivalent region of the pXen9 protein, AA 494–506: KNANPSESRYILV, by Neosystems (Paris). After primary screening to confirm that the serum gave an appropriate pattern of staining by comparison with NASE antibodies, the NPSE antibodies were affinity purified against the immunizing peptide by Dr. K. Herrenknecht of Eisai Laboratories (UCL). We are grateful to Dr. Herrenknecht for his generous assistance.

For protein extraction, *Xenopus* embryos (about 40) at stages 9, 20, and 35 were homogenized in 1.5 ml of extraction buffer (10 m*M* Hepes, pH 7.9, 83 m*M* NaCl, 1 m*M* $MgCl_2$), with freshly added protease inhibitors: 1 m*M* PMSF (phenylmethylsulfonyl fluoride) and 30 μg/ml each of antipain, pepstatin, and leupeptin (Sigma). Adult tissues (*Xenopus* kidney and rat brain) were treated similarly. The homogenates were kept on ice between spins to minimize sample breakdown. Homogenates were spun at 1000*g* for 10 min at 4°C, and the supernatants were transferred to fresh tubes and spun again at 1000*g* for 10 min at 4°C to remove yolk platelets and pigment granules. The supernatants were then spun at 10,000*g* for 20 min and the pellets were resuspended in 10 μl extraction buffer. Ten microliters of 2× loading buffer (10% β-mercaptoethanol, 20% glycerol, 4% SDS, 0.002% Bromophenol blue in 0.125 *M* Tris–HCl, pH 7.5) was added to each sample, and samples were heated at 65°C for 5 min, spun briefly at 11,600*g*, and stored at −20°C until loaded. For Western blotting, protein samples (40 or 60 μg per lane) were run on a 10% polyacrylamide gel and then transferred to Hybond-N+ (Amersham) in a Bio-Rad transfer apparatus. The membranes were blocked with 4% fat-free milk or 10% fetal calf serum in Tris-buffered saline, pH 7.4, for 2 hr and stained with NPSE or NASE antibodies at 1:50. Bound antibodies were detected with biotinylated anti-rabbit antibodies followed by peroxidase-coupled streptavidin (Vector). The peroxidase stain was developed with 1 mg/ml diaminobenzidine in 0.1 *M* Tris–HCl, pH 7.2, with freshly added 1% nickel chloride and 0.02% H_2O_2. Alternatively bound antibodies were detected with ^{125}I-labeled protein A (Amersham), and the filter was washed and exposed to X-ray film.

Immunocytochemical localization of Na pump protein. Unfixed embryos were stripped manually of jelly coats and vitelline membranes, embedded in OCT, frozen in isopentane at −70°C, and sectioned at 8–10 μm on a Bright cryostat. Sections were collected on gelatinized slides, allowed to air dry, and stained within 2 hr with the following schedule: (i) 5 min in ice-cold methanol to permeabilize; (ii) 30-min wash in 0.1 *M* PO_4 buffer, pH 7.5; (iii) 30 min in blocking serum (1% normal goat serum (GIBCO) + 1% fetal calf serum (GIBCO)) followed by 2 × 10-min washes in buffer; (iv) overnight at room temperature in primary antibody appropriately diluted in 0.1 *M* PO_4 buffer, pH 7.5, followed by 2 × 10-min washes in buffer; (v) 2–3 hr at room temperature with 1:100 diluted biotinylated goat anti-rabbit antibody (Vector) in 0.1 *M* PO_4 buffer, pH 7.5, followed by two further 10-min washes in buffer; and (vi) 2–3 hr at room temperature with FITC–streptavidin (1:600; Vector) in 0.1 *M* PO_4 buffer, pH 7.5. After a final 15-min wash in 0.1 *M* PO_4 buffer, sections were mounted in Citifluor (City University) to reduce fading. Sections were examined on a Zeiss microscope equipped with incident fluorescence and photographs were taken with Kodak Tri-X Pan 400. Results are based on examination of at least five embryos of the appropriate stage. NASE and NPSE antibodies gave virtually identical patterns of staining and are not described separately (Fig. 1). For controls, either primary antibody was omitted from the staining schedule or the peptide used to raise the antibodies was included with primary antibody.

Antibodies specific for α_2 (HERED) and α_3 (TED) sodium pump isoforms also were tested for the ability to stain *Xenopus* embryos (kindly donated by Professor Pressley and described in Pressley, 1992).

RESULTS

The sequence of the pXen9 cDNA is given in Fig. 2A. The clone is 3380 nucleotides long with a 3069-nt open

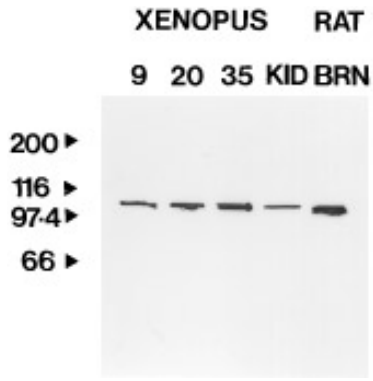

FIG. 1. Western blot of protein extracts from *Xenopus* embryos at stage 9 (lane 1), stage 20 (lane 2), stage 35 (lane 3), adult *Xenopus* kidney (lane 4), and rat brain (lane 5) probed with NPSE antibodies. Sixty micrograms of protein was loaded per lane. Note that in all cases the antibodies recognize a band at a molecular mass of about 100 kDa, which is appropriate for the predicted size of pXen9 protein. Molecular weight markers are shown to the left with arrowheads.

reading frame (ORF) and 276 nucleotides of 3′-noncoding sequence with a consensus polyadenylation signal at nucleotide 3354. The cDNA encodes a 1023 amino acid protein, which shares greatest homology with α_1 subunit isoforms (see Felsenfeld and Sweadner, 1988) and has a predicted molecular mass of 113 kDa. It has the lysine-enriched 5′ region found in all Na pump cDNAs so far sequenced. Immediately after the lysine box, at position 94 in the ORF, there is a second start signal, with six other putative start signals in the first 166 amino acids of the ORF, giving the opportunity for the production of 5′-truncated forms of the protein.

pXen9 shares high homology with the α_1 subunit clone isolated from the A6 *Xenopus* kidney cell line (Verrey *et al.*, 1989). However, the two clones are not identical. Figure 2B compares the nucleotide sequence of pXen9 with the A6 clone at the 5′ end, where the greatest difference is found. Relative to the A6 clone, the 5′ noncoding region of pXen9 shows a 2-base deletion, 3-base substitutions, and a 4-base insertion 10 bases upstream from the first start codon. In the lysine box region of the ORF, 6 bases are deleted in pXen9 relative to A6, so that pXen9 has only two Gly Lys pairs compared to the three present in the A6 clone. There are 13 other base substitutions in the ORF, all of which lie in the third base of the codon triplet. Consequently the remainder of the pXen9 protein is identical to the A6 clone. Where 3′-nontranslated region matching sequence is available for comparison, the two clones are identical.

A search for A6 mRNAs and other α isoforms of the sodium pump was made at neurula stages with reverse transcription in combination with the polymerase chain reaction (RT-PCR) to amplify the 5′ end of sodium pump message. A 3′ oligonucleotide primer was designed against a region of the sodium pump cDNA which is highly conserved in all isoforms (bases 506–523 in pXen9). 5′ primers were either common to both the A6 kidney cell line cDNA (Verrey *et al.*, 1989) and pXen9 (the first 16 bases of the ORF of pXen9) or A6-specific (the first 22 bases of the A6 cDNA; Verrey *et al.*, 1989). Two clones for a 490-bp PCR product amplified from stage 20 RNA proved to be identical, partial cDNAs for a sodium pump α subunit. The clone was most homologous to α_1 type isoforms and showed the lysine box characteristic of pXen9 rather than the A6 clone. However, there were significant differences from pXen9, with 20 nucleotide substitutions in the first 490 nucleotides, resulting in seven amino acid changes (Fig. 2C). One of these substitutions abolished the second putative start signal present in pXen9. No clones with the three Gly Lys pairs characteristic of the A6 cDNA were identified. Other α subunit isoforms also were not detected.

Temporal Expression of pXen9

The expression of pXen9 was followed from early cleavage stages through to stage 26 using dot blot analysis, Northern blotting, and RNase protection assay. For dot blot analysis and Northern blotting, samples were probed with full-length pXen9. A 200-nt probe (bases 321–521) was used for RNase protection assays.

Dot blot analysis of total RNA showed low signals prior to gastrulation and increasing signals from stage 10.5 onward. Northern blotting was less sensitive and convincing signals were not usually seen until stage 12, by which time neural induction is complete. Figure 3A shows Northern analysis for poly(A)$^+$ RNAs probed with full-length pXen9 from stage 10.5 (early gastrula) to stage 20, when the neural tube has just closed. No signal was detected at stage 10.5. Clear signals were detected at stages 12, 14, 17, and 20. Comparison with molecular weight markers put this band at 3.4 kb.

In RNase protection assays, Na pump α_1 subunit mRNAs were detected with the 200-nt 20us6 probe as a single band of the appropriate size at all stages examined; an example is shown in Fig. 3B. This implies that the start signal for any 5′-truncated RNAs is likely to lie 5′ to position 321 in the pXen9 cDNA. The Na pump α_1 subunit mRNA signal was compared with that for an ODC probe. Figure 3C plots signals from several experiments in which Na pump α_1 subunit mRNAs were determined from the 2- to 4-cell stage through to stage 26 and normalized relative to the ODC signal. Between the 2-cell and the blastula stages, the signal was very low. On average, Na pump α_1 subunit mRNAs doubled between the 2- to 4-cell stage and the early blastula stage (approx 2 hr) and increased again between the early and late blastula stages. The signal was still very low at the beginning of gastrulation and the first substantial increase occurred during gastrulation (stages 10.5 to 12) (P vs stage 9 = 0.009; Mann-Whitney test). Between stages 12 and 14, when the neural folds begin to lift, the level of Na pump mRNAs rose sharply and at stage 14 Na pump α_1 subunit mRNAs were about 10 times higher than that observed at

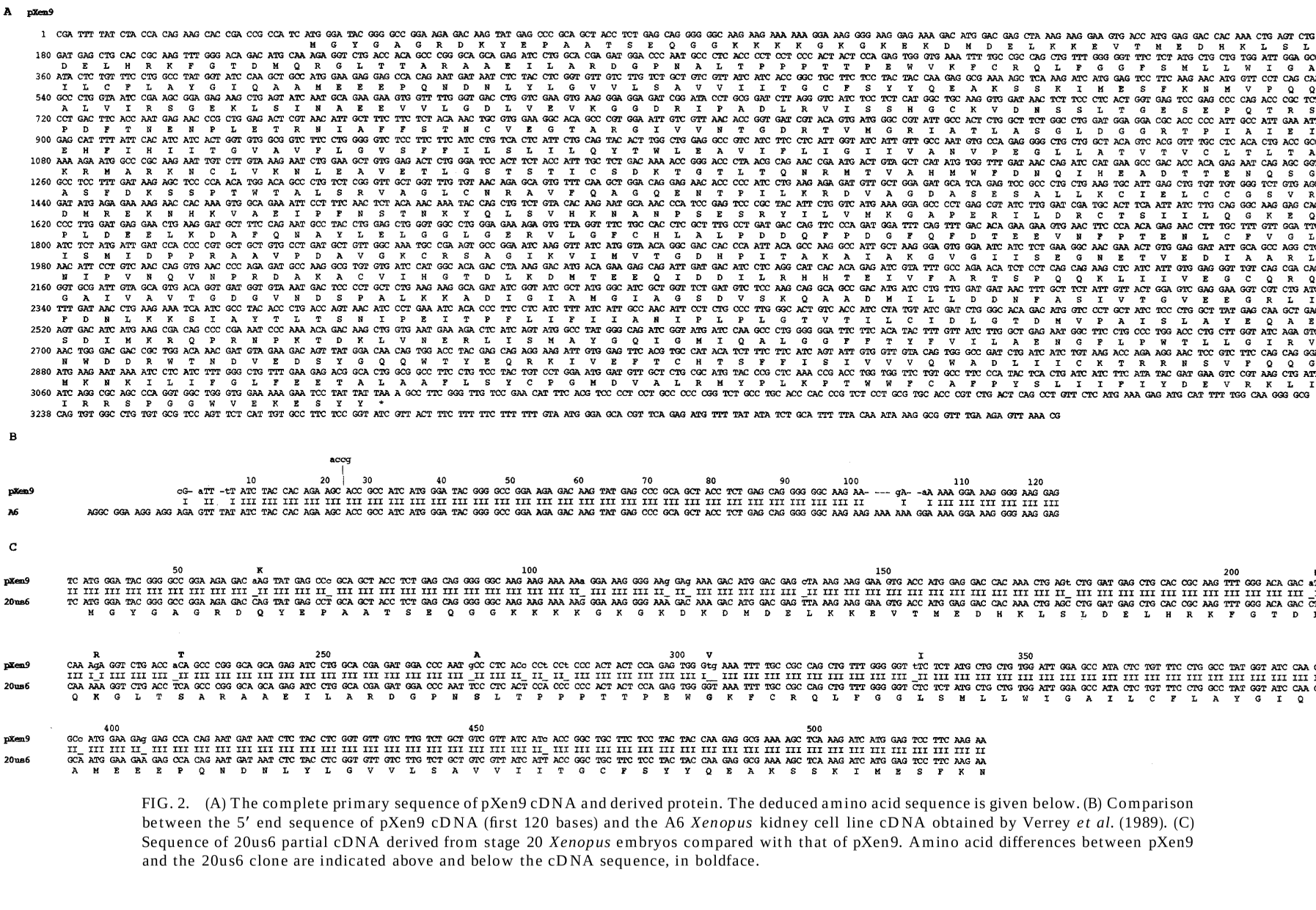

FIG. 2. (A) The complete primary sequence of pXen9 cDNA and derived protein. The deduced amino acid sequence is given below. (B) Comparison between the 5′ end sequence of pXen9 cDNA (first 120 bases) and the A6 *Xenopus* kidney cell line cDNA obtained by Verrey *et al.* (1989). (C) Sequence of 20us6 partial cDNA derived from stage 20 *Xenopus* embryos compared with that of pXen9. Amino acid differences between pXen9 and the 20us6 clone are indicated above and below the cDNA sequence, in boldface.

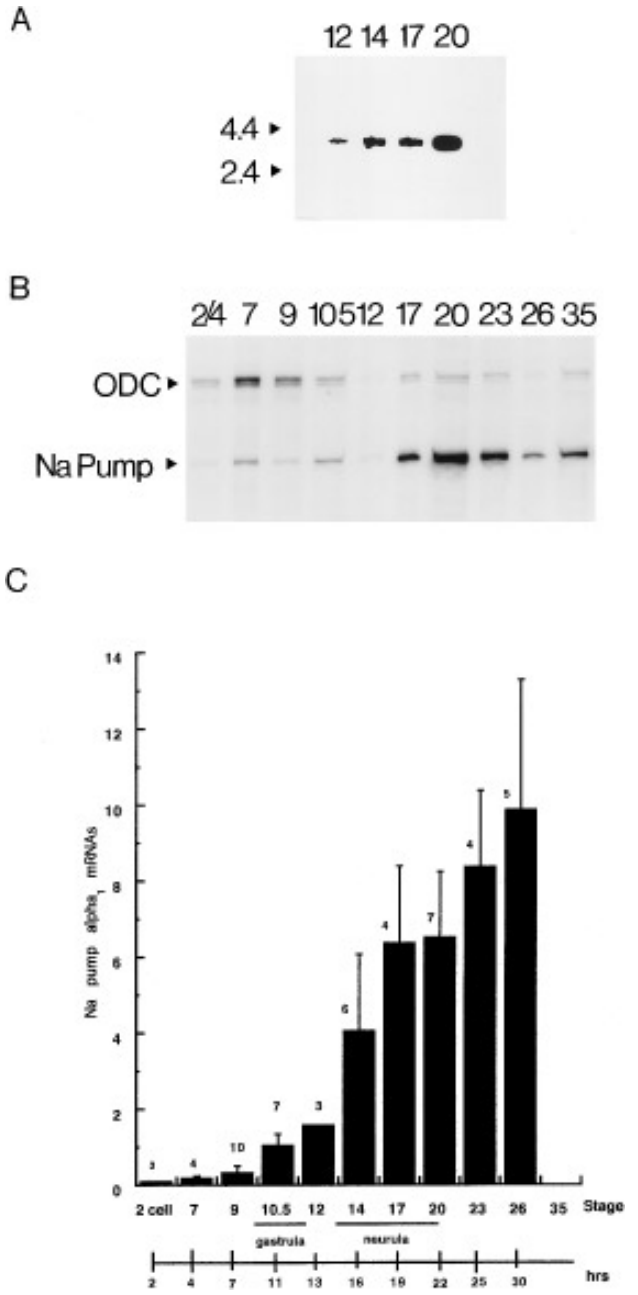

FIG. 3. The time course of expression of pXen9 RNAs. (A) Northern blot of poly(A)$^+$ RNAs from neurula stage *Xenopus* embryos probed with full-length pXen9. A sample at stage 10.5 run in the same experiment did not bind pXen9. Note clear signal at stage 12, which increases in intensity during neurulation. (B) Expression of pXen9 RNAs during development followed by RNase protection assay with the 20us6 probe. (Top band) ODC signal; (bottom band) 200-nt protected pXen9 fragment. Note that in this experiment the RNA loading at stage 12 was very low. (C) Time course of expression of pXen9 RNAs during development summarized from several experiments of the kind illustrated in B. The α subunit RNAs were detected with the 20us6 probe and in each experiment were normalized relative to the intensity of an ODC probe. Ordinate: α_1 subunit mRNAs (relative units). Abscissa: upper, Nieuwkoop and Faber developmental stage; lower, time after fertilization (hr). The number of determinations at each stage is given above each column. Bars, standard error of the mean, calculated when $n > 3$.

stage 9 (P vs stage 9 = 0.003). The average level of expression then continued to increase, although at a lower rate, up to stage 26. At these later stages the precise time course of the increase varied from batch to batch (indicated by the standard errors on the means). Consequently, even the increase by a factor of 2 in mean expression level between stages 14 and 26 was barely significantly different ($P = 0.06$).

Spatial Expression of pXen9 mRNAs

Although RNase protection analysis allows the time course of expression of pXen9 RNAs to be determined, it proved more useful to define the spatial expression pattern by *in situ* hybridization. Dissection of embryos into different regions was not informative because the Na pump is involved in a variety of developmental processes in both dorsal and ventral regions of the embryo. In dorsal structures it is important for the nervous system, while in the ventral part of the embryo the sodium pump drives expansion of the archenteron. Transport across the surface epithelium also will involve the Na pump. Since the expansion of the archenteron begins during the neurula stages, the substantial increase in Na pump mRNAs found in neurulae could derive as much from increased activity in ventral regions as from a rise in activity in the nervous system.

Whole mounts revealed widespread transcript expression, but were not useful for detailed analysis because of the density of phosphatase product (used to recognize transcript binding of anti-digoxygenin antibodies; see Materials and Methods) in the ectoderm. After hybridization as whole mounts, therefore, embryos were embedded in methacrylate resin and sectioned at 7 μm.

Figure 4 shows sections through 2-cell (A), 4-cell (B), 64-cell (C and D) and blastula stage (F, G, and H) embryos, when total mRNA expression is very low, together with sense controls (E and I). The most striking feature was the asymmetry in pXen9 transcript distribution, with levels highest at the animal pole, declining toward the equatorial regions, and almost completely absent in the vegetal pole. At the 2- and 4-cell stages, when the cells are very large, this gradient was apparent across single cells, with expression extending some way into the cell from the animal pole but little expression elsewhere. A striking feature at the 2-cell stage was the internal organization of α_1 subunit expression, which outlined large, apparently vesicular regions of the cytoplasm (Fig. 4A). Such ''vesicular'' structures were observed also at the 4-cell stage (Fig. 4B), although they were less prominent, but they were not observed at later stages. There is no ready explanation for this distribution pattern, which was not seen in sense controls (Fig. 4E).

As cleavage proceeded, a gradient of α_1 subunit mRNAs was maintained and the area over which Na pump mRNAs were detected remained roughly constant. At the 64-cell stage Na pump mRNAs were detected in the outermost animal pole cells (Fig. 4C) and gradually declined toward deep vegetal pole cells where expression was weak and limited to perinuclear regions (Fig. 4D). At the blastula stage transcript expression remained most marked in the outermost cells at the top of the animal pole (Fig. 4F, stage 7). The cells lining the blastocoel express lower levels of transcript (Fig. 4G). A similar decline occurred toward the equatorial region of the embryo (Fig. 4H, stage 9), and in the vegetal pole, mRNA expression was very weak, although still visible in perinuclear regions of the cell. To confirm this pattern, measurements were made also by direct hybridization to frozen sections. These results also revealed an asymmetry in Na pump α_1 subunit mRNAs from animal to vegetal pole.

At gastrulation, when the first marked increase in total α_1 subunit mRNAs was detected, the pattern of expression changed substantially. Figure 5A shows the dorsal side of the yolk plug in an embryo at stage 10.5, when gastrulation is underway. α_1 subunit transcripts are no longer detectable in the outermost dorsal ectoderm, which is destined to form the superficial layer of the neural plate. This pattern was retained as gastrulation continued (Fig. 5B, stage 11). The boundary between expressing and nonexpressing outer ectoderm cells (arrows) roughly coincided with the limit of invagination of the dorsal mesoderm. Figures 5C and 5D compare the dorsal and ventral sides of the yolk plug in an embryo at stage 12.5. The nonexpressing outer ectoderm cells now stretch back to include the whole of the future neural plate. The deep ectoderm layer shows intense Na pump α_1 subunit expression. Invaginating mesoderm cells show clear, although less substantial, mRNA expression and endoderm cells show virtually no expression other than in perinuclear regions. By contrast, on the ventral side of the yolk plug both layers of the ectoderm and the mesoderm express α subunit mRNAs at much the same level. Expression is apparent also in some endoderm cells.

Transverse sections through dorsal structures at stages 14 and 17, which encompass the major increase in Na pump mRNAs detected in RNase protection assays, are shown in Figs. 5E and 5F. At both stages, the deep layer of the neural plate expressed very high levels of Na pump α_1 subunit transcripts. Expression returned in the superficial layer of the neural plate. Both notochord and somites expressed Na pump α_1 subunit mRNAs at a relatively uniform level, which was lower than that in the neural plate. Endoderm cells, which now surround the expanding archenteron, show weak Na pump α_1 subunit expression. In the ectoderm expression remains high.

Once the neural tube has closed, neural tube cells and ectoderm cells continue to express Na pump mRNAs. Expression is more or less uniform in all dorsal structures (Fig. 5G, stage 22) and increases in intensity as development continues (Fig. 5H, stage 36). The final panels of Fig. 5 show a sense control at stage 17 (I) and embryos probed at stage 35 for Type II collagen (J) and actin (K) mRNAs. Both these probes reveal the expected tissue-specific expression pattern, with collagen mRNAs present in the notochord and floor plate, while actin is restricted to the somites.

Spatial Expression of Na Pump Protein

Two α_1-specific anti-peptide antibodies, NASE (Pressley, 1992) and NPSE, raised against the equivalent *Xenopus*-specific sequence and affinity purified against the immunizing peptide, were used to detect α_1 subunit protein. NPSE antibodies recognized a band of the same size as that identified by NASE antibodies in Western blots of protein extracts of *Xenopus* embryos, *Xenopus* kidney, and rat brain. Figure 1 shows a Western blot with NPSE antibodies of embryos at stages 9 (lane 1), 20 (lane 2), and 35 (lane 3), together with

FIG. 4. The spatial distribution of pXen9 mRNAs prior to gastrulation. Methacrylate sections through embryos that had been hybridized with a whole mount *in situ* schedule (see Materials and Methods). (A) 2 cell. (B) 4 cell. nuc, nuclei which have been lost during sectioning because of their very large size. (C) 64-cell, animal pole (AP). (D) 64-cell, vegetal pole (VP). (E) Sense control, 2 cell. (F) Outermost animal pole cells at stage 7. (G) Animal pole cells lining the blastocoel (blast) at stage 7 (early blastula). (H) Equatorial region of stage 9 (late blastula) AN, animal pole; VEG, vegetal pole. blast, blastocoel. (I) Sense control: stage 7. Bars, 100 μm.

FIG. 5. The spatial distribution of pXen9 RNAs during gastrulation and neurulation. (A) Longitudinal section through the dorsal lip of an early gastrula (stage 10.5). Note absence of signal in outer layer of dorsal ectoderm behind the dorsal lip, with a sharp boundary between nonexpressing and expressing cells (arrow). The nonexpressing cells are destined to form the outer layer of the neural plate. DL, dorsal lip. (B) Embryo at stage 11. The region of nonexpressing dorsal ectoderm cells now extends further back (arrow), paralleling invagination of the mesoderm. (C, D) Longitudinal sections through dorsal (C) and ventral (D) regions of an embryo at the end of gastrulation (stage 12). Note the lack of expression in the outer layer of the dorsal ectoderm, the putative neural plate. DL, dorsal lip; VL, ventral lip; YP, yolk plug. (E) Stage 14, transverse section through the neural plate. Note transcript expression is lower in superficial cells than deep cells of the neural plate (NP). The notochord (no), somites (som), and endoderm cells lining the archenteron show transcript expression. (F) Stage 17. Expression is most intense in the neural plate (NP) and lateral ectoderm (LE). The notochord (no) and somites (som) now show more intense expression than endoderm cells lining the expanding archenteron. (G) Stage 22. NT, neural tube; no, notochord; som, somites. (H) Stage 36. All dorsal structures now show intense expression of Na pump α_1 subunit mRNAs. (I) Sense control, stage 17. (J) Stage 36; expression of collagen mRNAs. Note expression restricted to the notochord and floor plate (FP). (K) Stage 36. Expression of actin mRNAs is restricted to the somites. Bars, 100 μm for all except H, J where bars are 25 μm.

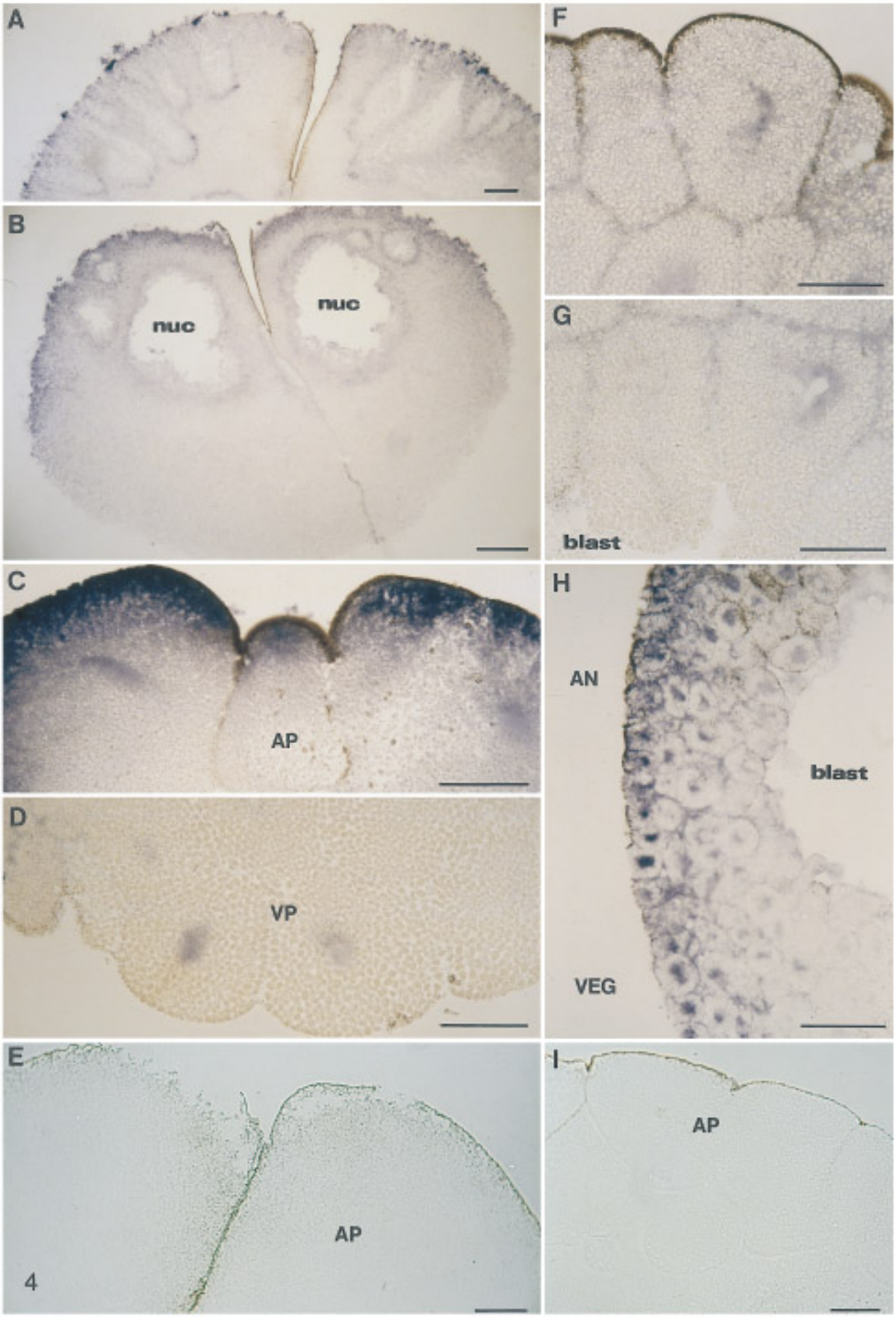
A
B
nuc
nuc
C
AP
D
VP
E
AP
4
F
G
blast
H
AN
blast
VEG
I
AP

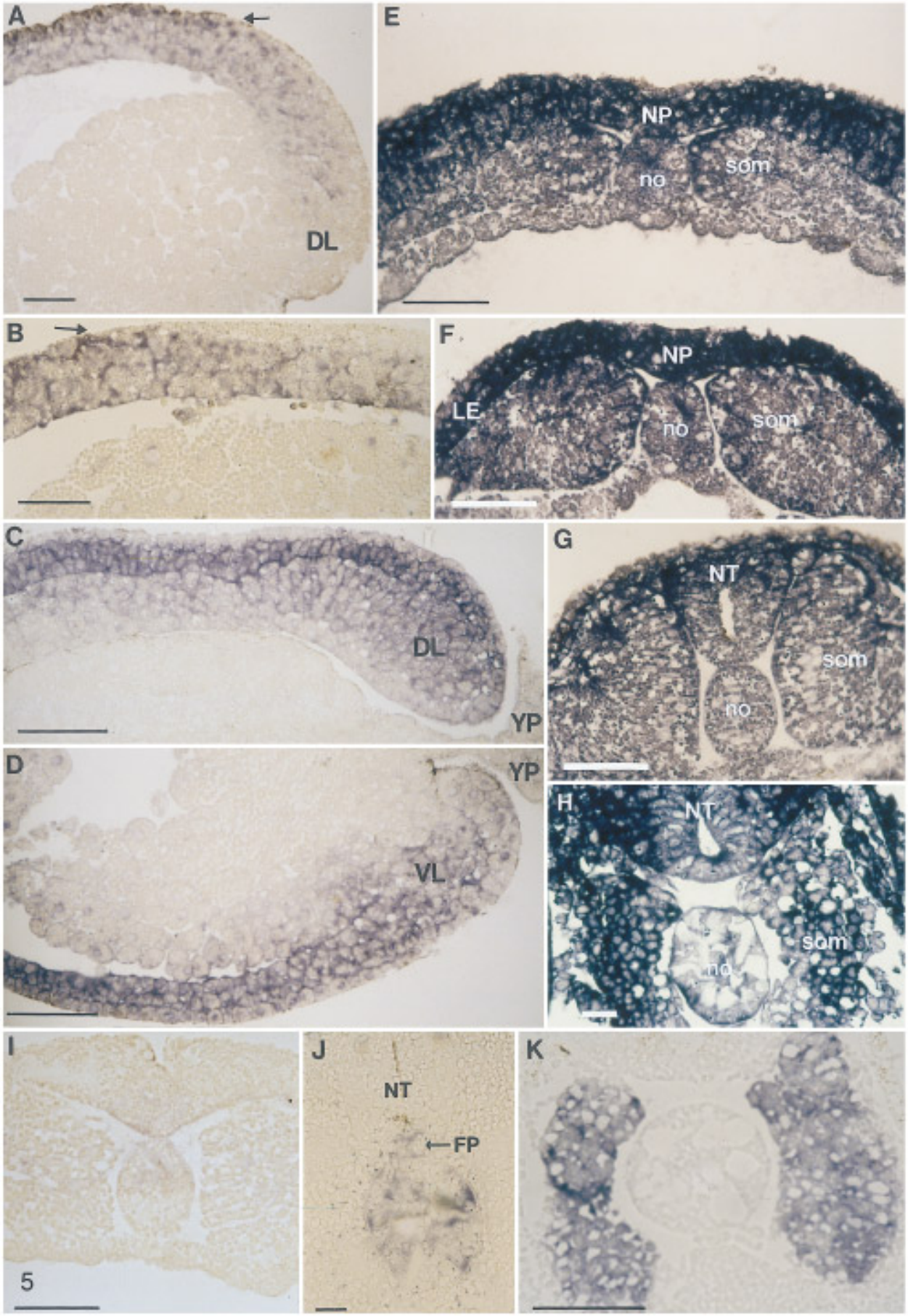
A
DL
E
NP
no
som
B
F
NP
LE
no
som
C
DL
YP
G
NT
som
no
D
YP
VL
H
NT
som
no
I
5
J
NT
FP
K

samples of Xenopus kidney (lane 4) and rat brain (lane 5). In all samples the antibodies recognized a major band of just below 116 kDa, close to the size predicted from the pXen9 ORF. This band was approximately the same size as that identified previously as α_1 subunit protein in rat brain (Pressley, 1992). A low abundance, lower molecular weight band was sometimes apparent, which would be compatible with a 5′-truncated protein generated from one of the early putative start signals. Both antibodies gave identical patterns of immunocytochemical staining and they are not described separately.

Prior to gastrulation all cells expressed the α_1 subunit protein. Figure 6 shows that in outer animal pole cells, the sodium pump was located predominantly on the lateral and basal membranes of the cell (Fig. 6A, 4-cell stage; Fig. 6B, 64-cell stage; Fig. 6D, early blastula). This polarized distribution is characteristic of transporting epithelia and is consistent with models for the formation of the blastocoel (Slack and Warner, 1973). As cleavage proceeded, protein was detected also in deep cells in the animal pole, where antibody staining was detected over the whole cell surface (Fig. 6C, 64-cell stage, cells facing the blastocoel; Fig. 6E, early blastula, cells facing the blastocoel). Vegetal pole cells at the early blastula stage (Fig. 6F) and deep cells in the equatorial region at the late blastula stage (Fig. 6G) expressed the α_1 subunit on all surface membranes. In single sections the stain around individual cells was often patchy, rather than continuous.

Figure 7 shows sections through gastrulating embryos, when a marked change in distribution of Na pump α_1 subunit protein occurred. Figures 7A and 7B show the developing blastopore in two early gastrulae. Intense stain is apparent on the apical surfaces of outer ectoderm cells in the region of the blastopore on both the dorsal and ventral sides. Sections taken at stage 12 from a single embryo through the outer edge of the yolk plug (Fig. 7D) and at the point where invaginating endoderm cells are moving into the embryo (Fig. 7C) reveal dense staining for the sodium pump on the apical surfaces of the cells lining the blastopore and on the apposing surfaces of invaginating endoderm cells. Elsewhere endoderm cells showed little stain.

Figure 8 shows α_1 subunit protein expression in dorsal structures during neurulation. Sodium pump protein was first detected in rostral regions of the notochord at stage 13 (Fig. 8A). At stage 14, Na pump protein staining increased in the rostral notochord (Fig. 8B), while in caudal regions the notochord was still negative (Fig. 8C). Weak and patchy staining was observed occasionally on the basal surface of deep neural plate cells. There was no other obvious stain in dorsal structures at this stage, although lateral and ventral ectoderm cells continued to display sodium pump protein on their surface membranes. At stage 17 (Figs. 8D and 8E) superficial neural plate cells remained negative. However, stain along the basal side of deep neural plate cells was now prominent. This extended to the lateral margins of the neural plate and then stopped abruptly (Fig. 8, arrow). Floor plate cells, which share the origin of the notochord, also now stained with sodium pump α_1 subunit antibodies (example in Fig. 8F). Despite the presence of pXen9 mRNAs in the somites, there was insufficient Na pump α_1 subunit protein in the surface membranes to be detectable, except as occasional spotting.

At stage 20, when the neural tube had just closed, staining of the notochord remained prominent; however, neural tube cells were negative. Figure 9 shows sections through an embryo at stage 23, shortly after the neural tube had closed. Figure 9A shows the notochord, bottom of the neural tube, and top of the expanding archenteron. Staining for the α_1 subunit protein in the notochord was bright, probably because the adjacent cell membranes of the vacuolated cells were too close to be distinguished separately. Figure 9B shows a higher power image to illustrate the staining of the floor plate and apical surfaces of ventral neural plate cells lining the neurocoel, which are derived from the superficial layer of the neural plate. Figure 9C illustrates the dense staining of the cells facing the expanding archenteron. This pattern was retained at stage 35, illustrated here (Fig. 9D) for the ventral neurocoel and notochord. Stain was always most dense at the ventral side of the neurocoel, in cells flanking floor plate cells, which continued to express the sodium pump α_1 subunit, and in the notochord. Elsewhere in the embryo, the distribution of the sodium pump was as to be expected from the gradual expansion of the intercellular cavities and is not illustrated. Bright staining was retained on endoderm cells lining the expanding archenteron, and deep endoderm cells also began to express the protein on their surface membranes. With the formation of the pharynx, a similar pattern of Na pump α_1 subunit protein expression emerged, with cells lining the pharyngeal cavity showing the highest density of Na pump protein.

Antibodies specific for α_2 and α_3 isoforms (HERED and TED; Pressley, 1992) were tested on sections from the 2-cell stage up to stage 35, but failed to give convincing staining.

DISCUSSION

Physiological studies have revealed the functional importance of the sodium pump during early development, both in relation to the generation of embryonic, fluid-filled cavities (e.g., Slack and Warner, 1973; Biggers *et al.*, 1977) and in the control of neuronal differentiation (Blackshaw and Warner, 1976b; Messenger and Warner, 1979). The results presented here show the complementary patterns of expression of Na pump α_1 subunit mRNAs and integral membrane protein.

Two cDNAs, one complete, one partial, have been isolated for the α catalytic subunit of the sodium pump from the *Xenopus* embryo. Both clones show closest homology with α_1 isoforms and may be allelic forms. Other α_1 subunit isoforms were not detected. This could imply that only catalytic subunit isoforms of the α_1 subtype are present in the early *Xenopus* embryo. Alternatively, other α isoforms could be present but at levels that are sufficiently low to

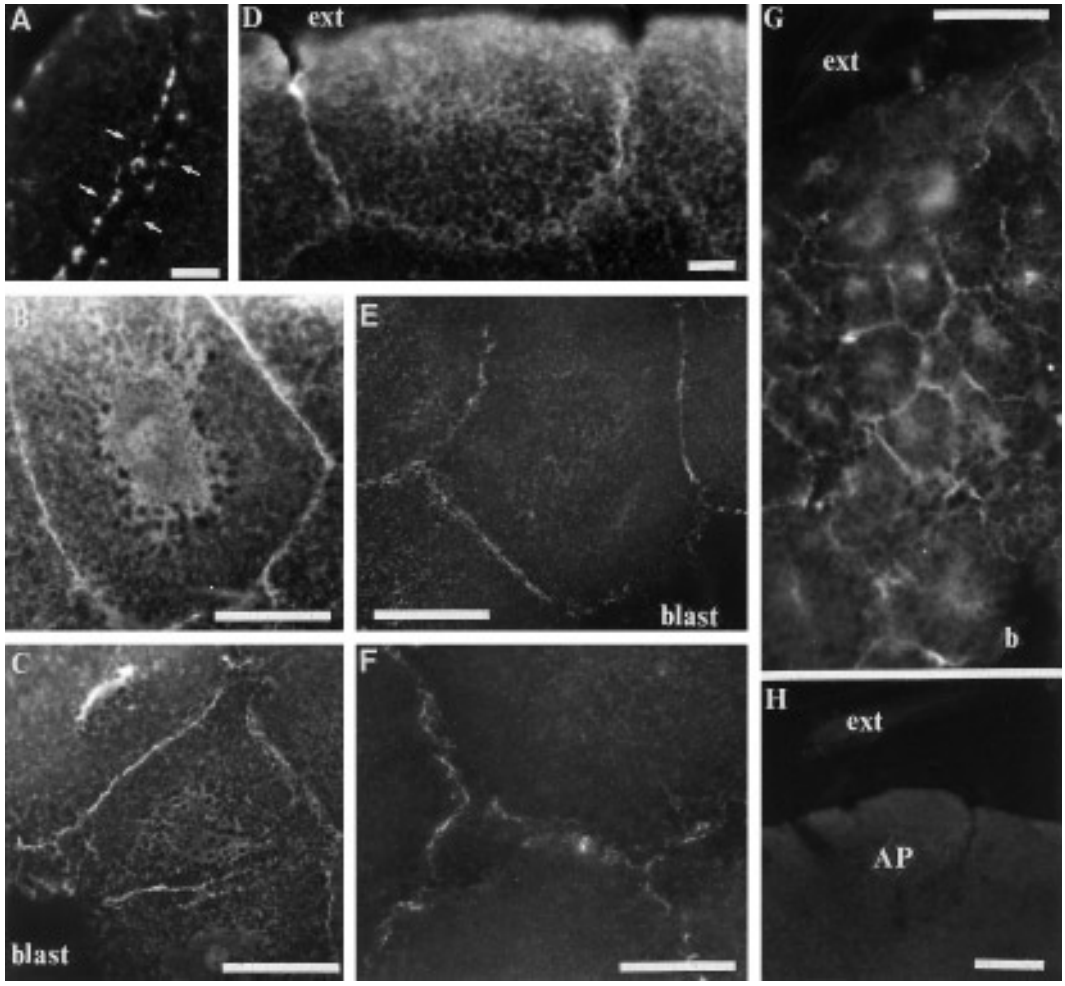

FIG. 6. The expression of Na pump α_1 subunit protein prior to gastrulation detected with NPSE or NASE antibodies. The relatively high background apparent in some images stems from inherent autofluorescence of the early *Xenopus* embryo. (A) Oblique section through embryo at the 4-cell stage. The cleavage furrow (indicated by arrows) stains intensely for α_1 subunit protein. (B) 64-cell stage; outer animal pole cells. Note stain restricted to lateral and basal regions of the cell. (C) 64-cell stage; animal pole cells lining the blastocoel (blast). (D) Stage 7, outer animal pole cells. ext, the outside of the embryo. α_1 subunit protein is limited to the lateral and basal membranes. (E) Stage 7, animal pole cells facing the blastocoel (blast). (F) Stage 7 deep vegetal pole cells. Note protein stain on all cell surfaces. (G) Stage 9, part of section through the embryo showing outer animal pole cells and cells facing the blastocoel. Protein stain is absent from the outer surface, but stain of varying intensity is present on all other cell membranes. ext, external surface of embryo. b, blastocoel facing surface. (H) Stage 7, antibody stain is abolished in the presence of competing peptide. ext, extraembryonic surface; AP, animal pole cells. Bars in A, B, D, 25 μm; in remainder, 100 μm.

make their detection difficult. The homology between the cDNAs for the *Xenopus* embryonic α_1 isoforms described here and the α_1 cDNA isolated previously from the A6 *Xenopus* kidney cell line (Verrey *et al.*, 1989) is high, although the clones are not identical. We were unable to detect a cDNA that matched the A6 clone precisely; all cDNAs isolated from embryonic material showed a 6-bp deletion in the lysine box region. Genomic clones with both lysine box patterns have been isolated (Davies, Patel, Messenger, and Warner, in preparation), which suggests that in the early embryo the two lysine box (pXen9) form may dominate. The homology between pXen9, p20us6, and A6 cDNAs and the α_1 subunit cDNA from *Bufo* (Jaisser *et al.*, 1992) also is high. Since the *Xenopus* sodium pump is ouabain-sensitive while that for *Bufo* is ouabain-resistant, do these comparisons provide clues about the region responsible for ouabain sensitivity? The only region showing significant differences between the *Bufo* clone and all three *Xenopus* clones lies at the H1–H2 extracellular loop boundary (AA 118–129 of pXen9) where five of the first six amino acids differ between *Xenopus* and *Bufo*, and this region might be responsible for the difference in ouabain sensitivity. The rat α_1 subunit also

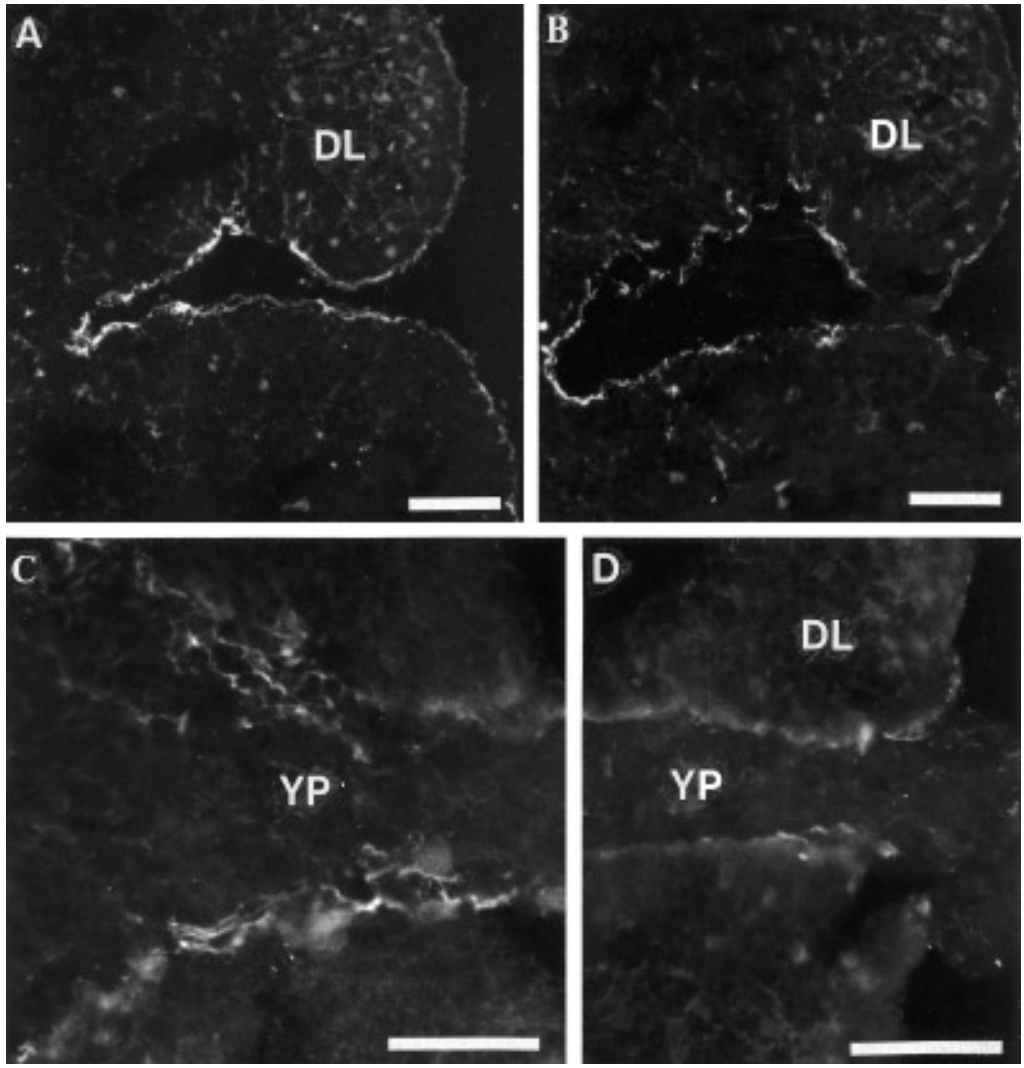

FIG. 7. The expression of α_1 subunit protein during gastrulation. (A, B) Sections through the dorsal lip of two embryos at the beginning of gastrulation. DL, dorsal lip. Note protein stain is limited to cells lining the developing blastopore. (C, D) Sections through two regions of the yolk plug of a single embryo at stage 12. DL, dorsal lip; YP, yolk plug. Note intense protein stain on the apposing surfaces of ectoderm and endoderm as cells move through the blastopore. This is particularly clear in C, which shows endoderm cells as they move into the embryo. Bars, 100 μm.

shows low sensitivity to ouabain. However, only the N-terminus arginine of the H1–H2 region is present in rat α_1 and *Bufo* clones, but not in *Xenopus.*

The description by Burgener-Kairuz *et al.* (1994) of the developmental time course of Na pump α_1 subunit mRNA expression obtained by Northern blotting of embryonic mRNAs with an A6 kidney cell line probe is consistent with that described with RNase protection assays in more detail here. This is not surprising since the homology between *Xenopus* embryonic mRNAs and an A6 probe is sufficiently high to allow efficient cross-hybridization.

Up to the late blastula stage, Na pump α_1 subunit mRNAs were detected at very low levels. Prior to the midblastula transition it is likely that this reflects maternal mRNAs, rather than zygotic transcripts. The increase observed during the blastula stages, when transcription of the embryonic genome first begins (Newport and Kirschner, 1982), could stem from *de novo* RNA synthesis. The gradual rise in mRNA expression followed the increase in cell surface membrane area generated by cell division and was matched by the appearance of Na pump α_1 subunit protein in the cell membranes. A very small rise in Na pump enzyme activity can just be detected during these stages of development and pooled embryos at stages 8–10 show up regulation of α subunit biosynthesis (Han *et al.,* 1991). Outer cells in the animal pole showed the Na pump distribution charac-

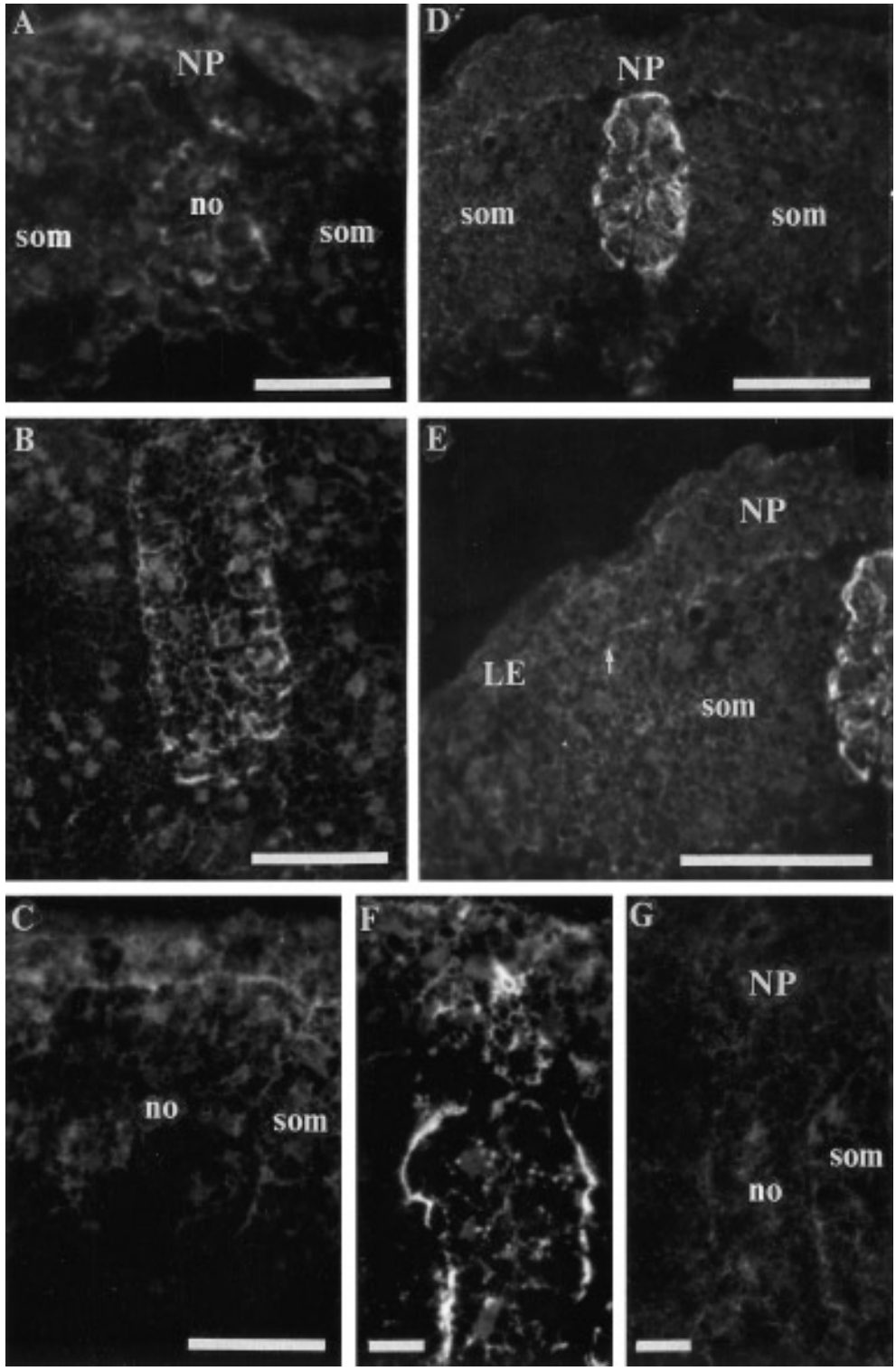

FIG. 8. The expression of α_1 subunit protein during neurulation. (A) Stage 13. The rostral notochord (no) begins to stain for α_1 subunit protein. The neural plate (NP) and somites (som) show little stain. (B) Stage 14, rostral. The notochord begins to show prominent staining for α_1 subunit protein. (C) Stage 14, caudal. Notochord staining (no) is absent. There is some patchy staining elsewhere. som, somites. (D) Stage 17. The deep surface of neural plate cells (NP) stain for α_1 subunit protein. The notochord stains intensely and the somites (som) show only weak and patchy stain. (E) Stage 17. The boundary (arrow) of α_1 subunit protein between deep neural plate (NP) and lateral ectoderm (LE) cells. Part of the intensely stained notochord is visible and the somite (som) shows little stain. (F) Stage 17: an example of α_1 subunit protein expression in floor plate cells lying immediately above the intensely staining notochord. (G) Stage 17. Negative control. NP, neural plate; no, notochord; som, somite. Bars, 25 μm for F, G; otherwise, 100 μm.

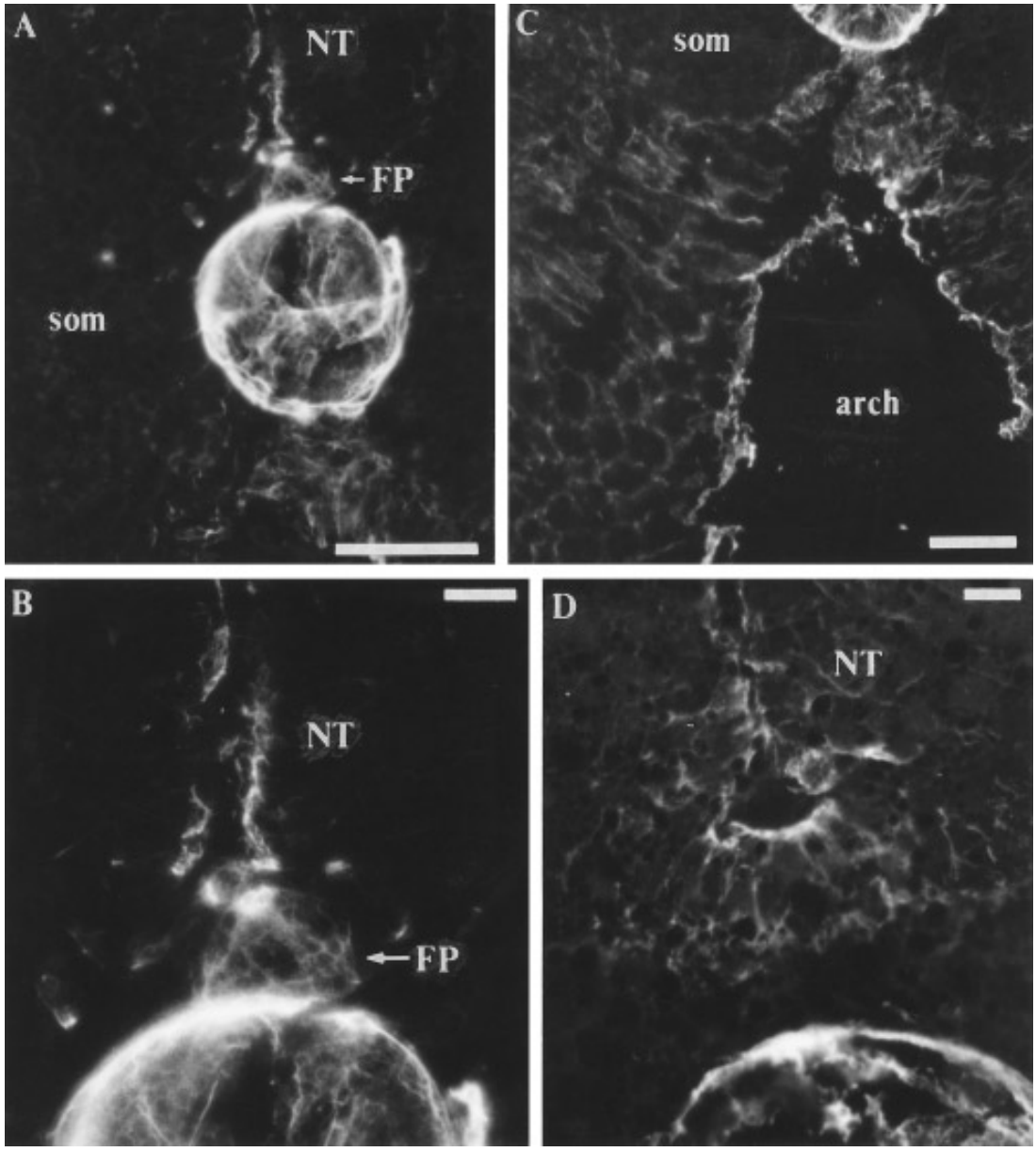

FIG. 9. The expression of α_1 subunit protein after closure of the neural tube. (A) Stage 22/23. Note intense stain of notochord, floor plate (FP), and apical surfaces of neural tube cells (NT). som, somites. (B) Enlargement of A to show the region just above the notochord to further illustrate floor plate (FP) and neurocoel lining stain. NT, neural tube. (C) Ventral region of same section to show pattern of α_1 subunit protein expression in the expanding archenteron (arch). The ventral side of the notochord is just visible. The somites (som) continue to show little expression. (D) Stage 36. The dorsal notochord and ventral region of the neural tube (NT). Note marked expression along the cell surfaces lining the neurocoel, particularly in the floor plate. (A, C) Bar, 100 μm; (B, D) Bar, 25 μm.

teristic of cells engaged in vectorial fluid transport across epithelia, with little at the apical surfaces and high levels in the lateral membranes behind the tight junctions that seal the intercellular spaces from the extraembryonic fluid.

The first clear increase in Na pump α_1 subunit mRNAs occurred during gastrulation. This was accompanied by a shift in the spatial pattern of expression of both mRNAs and protein. mRNA expression in endoderm cells remained very low and surface membrane protein in endoderm cells that had moved through the blastopore remained at or below the immunocytochemical detection level. Mesoderm cells expressed high levels of mRNAs. However, the most

striking feature was the alteration in distribution of both Na pump α_1 subunit mRNAs and protein at the blastopore. Na pump protein was detected at high density on the apical surfaces of cells lining the blastopore and on the apposing membranes of invaginating yolk plug cells. This suggests that the entry of fluid during gastrulation from the dilute bathing medium into the embryonic intercellular spaces may be opposed by localized high activity of the sodium pump at the blastopore. During gastrulation, the concentration of Na in the interstitial fluid falls from about 100 to 70 m*M*, to return to 100 m*M* once gastrulation is over (Gillespie, 1983). In the ectoderm, Na pump mRNAs and protein were barely detectable in those outermost dorsal ectoderm cells destined to become the surface layer of the neural plate. The region showing low mRNA expression matched the progress of the invaginating mesoderm, stretching further along the embryonic axis as gastrulation proceeded. Elsewhere outer ectoderm cells retained Na pump-free apical surfaces and Na pump-dense lateral membranes.

A sharp, and substantial, increase in Na pump α_1 subunit mRNAs occurred between stages 12 and 14, which encompass the early steps in neurulation and the first expansion of the archenteron. *In situ* hybridization revealed that Na pump mRNAs increased in all dorsal structures, in the lateral and ventral mesoderm, and in endoderm cells lining the developing archenteron. However, the distribution of Na pump α_1 subunit protein at sufficient density to be detected was highly restricted, particularly in dorsal structures. At stages 13, 14, and 17, no protein was detectable in surface neural plate cells, reflecting the marked reduction in Na pump mRNAs in these cells during gastrulation and implying that Na pump α_1 subunit protein expression is down-regulated in superficial neural plate cells. A surprising, and striking, finding was the appearance of dense protein staining in the notochord, which first became apparent at stage 13, was pronounced in rostral regions at stage 14, and was then maintained at a high level along the length of the notochord up to stage 35, the latest stage examined. Notochord staining was paralleled by stain of floor plate cells. The significance of this high expression of the sodium pump in the notochord is not known. Staining in flanking myotomal cells was, by contrast, weak and patchy. Myotomal muscle cells attain high resting membrane potentials before segmentation begins (Blackshaw and Warner, 1976a), which implies both relatively low membrane conductance and efficient Na pumping. Presumably the Na pump density in myotomal cell membranes was too low to be detected readily by antibody staining.

Han *et al.* (1991) used methionine labeling and immunoprecipitation to follow the biosynthesis of total Na pump α subunit protein during early development of *Xenopus laevis* and deduced that most new biosynthesis of α subunit protein occurs between stages 16 and 21, during the mid to late neurula stages. The increase in total protein levels was of the same order as that observed here for α_1 subunit mRNAs. A substantial increase in α subunit protein detected with both their Aα and their Aα_1N antibodies occurred at stage 13, with a further increase during neurulation. Although these measurements were not made at precisely the same stages as the mRNA levels reported here, the two time courses are entirely compatible.

Functional studies (Blackshaw and Warner, 1976b) have shown that additional sodium pumps are inserted into the membranes of neural plate cells from stages 14–15 onward. Patchy protein staining along the basal surface of deep neural plate cells was observed in some embryos as early as stage 14. The increase in resting membrane potential of neural plate cells associated with the insertion of these additional sodium pumps is complete by about stage 17 (Blackshaw and Warner, 1976b) and in stage 17 embryos the basal surfaces of deep neural plate cells always stained for sodium pump α_1 subunit protein. Stain stopped at the lateral margins of the neural plate, which matches the physiological observation that only neural plate cells show a sodium pump driven increase in membrane potential (Blackshaw and Warner, 1976b). Na pump protein expression also was detected at about stage 17 in the midline precursors of the floor plate. Sodium pumps in floor plate cells could contribute to the Na pump driven alterations in membrane potential in the neural plate.

The present experiments do not suggest that the sodium pumps associated with neural plate development, and intimately involved in the process of neuronal differentiation (Messenger and Warner, 1979), reflect the appearance of a new α subunit isoform. We were unable to detect α subunit mRNAs other than those with the pXen9 lysine box. Antibody staining with isoform-specific antibodies suggest also that α isoforms other than the α_1 subtype are either not present or of very low abundance. TED (α_3) antibodies show wide cross-reactivity across species, both vertebrate and invertebrate (Pressley, 1992), and might be expected to detect an α_3 or α_3-like isoform in *Xenopus;* no convincing immunostaining was observed. Pressley noted that HERED antibodies, while less widespread in their cross reactivity than TED antibodies, detected α_2 or α_2-like isoforms in a wider range of species than the α_1-specific NASE. HERED antibodies gave no staining in *Xenopus,* while both the α_1-specific NASE and NPSE antibodies gave convincing staining. These observations raise the interesting question of the origin of the doublet of α subunit protein detected by Han *et al.* (1991) by differential immunostaining of Western blots. Their Aα antibodies, raised against purified α subunit from *Bufo marinus* kidney (Girardet *et al.*, 1981), detected a doublet of α subunit protein, which they speculate might reflect α subunit isoforms in addition to the α_1 subunit detected by Aα_1 antibodies, which were raised against the first 98 amino acids of the A6 *Xenopus* protein. One possibility is that the slightly larger protein detected by Han *et al.* (1991) reflects cellular accumulation of another α isoform that is not inserted into cell membranes at early stages of development. The α_1 subunit-specific antibodies used here were raised against AA 494–506 of pXen9, a region that is completely conserved between A6 and pXen9, and might therefore be expected to detect all forms of the α_1 subunit protein.

In addition to the major band of the size appropriate for pXen9, these antibodies occasionally detected a low-abundance protein of lower molecular mass which could suggest the presence of either 5′-truncated forms generated from one of the putative start signals or 3′-truncated forms of the protein.

Targeting of a functionally active sodium pump into the membrane requires association between α and β subunits, and some functional properties of the pump, such as sensitivity to the extracellular potassium concentration, can be modulated by an alteration in the β subunit (for review, see Chow and Forte, 1995). In this connection, it is interesting that Blackshaw and Warner's (1976b) results show that raising extracellular potassium to 20 m*M* at stage 131/2 initiates a precocious increase in resting membrane potential in the neural plate, but not in the ectoderm. One possibility is that the β_3 isoform that is first expressed at high levels during the neurula stages (Good *et al.*, 1990) controls the insertion of new sodium pumps into the membranes of neural plate cells. However, analysis by *in situ* hybridization with a β_3 probe (kindly donated by P. Good) shows that this β isoform is found predominantly in the endoderm and is excluded from the notochord and nervous system during these stages (N. J. Messenger and A. E. Warner, in preparation). Alternatively, neural plate-specific control sequences may activate transcription and subsequent insertion of additional Na pumps. Posttranslational control mechanisms also may play a part.

Once the neural tube has closed, Na pump α_1 subunit protein is no longer detected at the outermost borders of the neural tube, where differentiation of the first neurones begins at stages 21–23 (e.g., Blackshaw and Warner, 1976c; N. J. Messenger and Warner, 1989), although floor plate cells continue to stain strongly. Na pump α_1 subunit protein is now detected along the apical and lateral surfaces of cells lining the neurocoel, suggesting that the size of the neurocoel may be modulated by the activity of the sodium pump.

The other alterations in Na pump distribution match the generation of the internal cavities. Cells lining the archenteron express increasing levels of Na pump mRNAs and pump protein appears along the lateral membranes. Similarly, Na pumps appear along the borders of cells lining the developing pharynx, while outer ectoderm cells always maintain the pattern characteristic of cells in transporting epithelia engaged in vectorial fluid transfer.

The match between previous physiological observations on the functional roles played by the sodium pump during early development of the amphibian embryo and the mRNA and protein expression patterns for the α_1 subunit of the sodium pump described here is good. It will be interesting to determine the relationship between the activation of the sodium pump and the activation of genes such as *Xash-3* (see Ferreiro *et al.*, 1994), X-Delta-1, and Notch-1 (Chitnis *et al.*, 1995), which may play an important part in the progression from ectoderm to neural tissue initiated by neural induction. One possibility is that the sodium pump may be a downstream target of such genes, which could promote specifically sodium pump expression in the neural plate. The time course of expression of Na pump protein in the neural plate is consistent with such a suggestion since these genes appear to promote a neuronal fate and are detected (e.g., Zimmerman *et al.*, 1993) several hours before Na pumps are inserted into the membranes of neural plate cells.

ACKNOWLEDGMENTS

This work was made possible by a grant from the Wellcome Trust (19083/1.5). A.E.W. thanks the Royal Society for their support. We are grateful to J. Lingrel, C. Kintner, T. Pressley, and L. Dale for gifts of reagents and to L. Dale for advice. Dr. P. Gates gave valuable advice and assistance with the production of nested deletion clones.

REFERENCES

Ausubel, F., Brent, R., Kingston, R. E., Moore, D. D., Seidman, J. G., Smith, J. A., and Struhl, K. (1994). ''Current Protocols in Molecular Biology.'' Wiley, New York.

Biggers, J. D., Borland, R. M., and Powers, R. D. (1977). Transport mechanisms in the preimplantation mammalian embryo. *Ciba Found. Symp.* 18–20, 129–153.

Blackshaw, S. E., and Warner, A. E. (1976a). Low resistance junctions between mesoderm cells during development of trunk muscles. *J. Physiol.* 255, 209–230.

Blackshaw, S. E., and Warner, A. E. (1976b). Alterations in resting membrane properties during neural plate stages of development of the nervous system. *J. Physiol.* 255, 231–247.

Blackshaw, S. E., and Warner, A. E. (1976c). Onset of acetylcholine sensitivity and endplate activity in developing myotome muscles of *Xenopus*. *Nature* 262, 217–218.

Breckenridge, L. J., and Warner, A. E. (1982). Intracellular sodium and the differentiation of amphibian embryonic neurones. *J. Physiol.* 332, 393–413.

Burgener-Kairuz, P., Corthesy-Theulaz, I., Merillat, A-M., Good, P., Geering, K., and Rossier, B. C. (1994). Polyadenylation of Na^+–K^+-ATPase β_1 sub-unit during early development of *Xenopus laevis*. *Am. J. Physiol.* 266, C157–C164.

Chitnis, A., Henrique, D., Lewis, J., Ish-Horowicz, D., and Kintner, C. (1995). Primary neurogenesis in *Xenopus* embryos regulated by a homologue of the *Drosophila* neurogenic gene *Delta*. *Nature London* 375, 761–766.

Chow, D. C., and Forte, J. G. (1995). Functional significance of the β-subunit for Heterodimeric P-Type ATPases. *J. Exp. Biol.* 198, 1–17.

Felsenfeld, D. P., and Sweadner, K. J. (1988). Fine specificity mapping and topography of an isozyme specific epitope of the Na,K ATPase catalytic subunit. *J. Biol. Chem.* 263, 10932–10942.

Ferreiro, B., Kintner, C., Zimmerman, K., Anderson, D., and Harris, W. A. (1994). XASH genes promote neurogenesis in *Xenopus* embryos. *Development* 120, 3649–3655.

Gillespie, J. I. (1983). The distribution of small ions during the early development of *Xenopus laevis* and *Ambystoma mexicanum* embryos. *J. Physiol.* 344, 359–377.

Girardet, M., Geering, K., Frantes, J. M., Geser, D., Rossier, B. C., Kraehenbuhl, J. P., and Bron, C. (1981). The immunochemical evidence for a transmembrane orientation of both the Na+, K+ -ATPase sub-units. *Biochemistry* 20(23), 6684–6691.

Good, P. J., Richter, K., and Dawid, I. B. (1990). A nervous system-specific isotype of the β subunit of Na^+, K^+-ATPase expressed during early development of *Xenopus laevis*. *Proc. Natl. Acad. Sci. USA* 87, 9088–9092.

Han, Y., Pralong-Zamofing, D., Ackermann, U., and Geering, K. (1991). Modulation of Na,K-ATPase expression during early development of *Xenopus laevis*. *Dev. Biol.* 145, 174–181.

Harland, R. M. (1991). *In situ* hybridization: An improved whole-mount method for *Xenopus* embryos. *Methods Cell Biol.* 36, 685–695.

Isaacs, H. V., Tannahill, D., and Slack, J. M. (1992). Expression of a novel FGF in the *Xenopus* embryo. A new candidate inducing factor for mesoderm formation and anteroposterior specification. *Development* 114, 711–720.

Jaisser, F., Canessa, C. M., Horisberger, J. D., and Rossier, B. C. (1992). Primary sequence and functional expression of a novel ouabain-resistant Na,K-ATPase. The β subunit modulates potassium activation of the Na,K-pump. *J. Biol. Chem.* 267, 16895–16903.

Kintner, C. R., and Melton, D. M. (1987). Expression of *Xenopus* N-CAM RNA is an early response of ectoderm to induction. *Development* 99, 311–325.

Melton, D. A., Kreig, P. A., Rebagliati, M. R., Maniatis, T., Zinn, K., and Green, M. R. (1984). Efficient *in vitro* synthesis of biologically active RNA and RNA hybridization probes from plasmids containing a bacterial SP6 promoter. *Nucleic Acids. Res.* 12, 7035–7056.

Messenger, E. A., and Warner, A. E. (1979). The function of the sodium pump during differentiation of amphibian embryonic neurones. *J. Physiol.* 292, 85–105.

Messenger, N. J., and Warner, A. E. (1989). The appearance of neural and glial cell markers during early development of the nervous system in the amphibian embryo. *Development* 107, 43–54.

Newport, J., and Kirschner, M. (1982). A major developmental transition in early *Xenopus* embryos. II. Control of the onset of transcription. *Cell* 30, 687–696.

Nieuwkoop, P. D., and Faber, J. (1967). ''Normal Table of *Xenopus laevis* (Daudin).'' North-Holland, Amsterdam.

Phillis, J. W., and Wu, P. H. (1981). Catecholamines and the sodium pump in excitable cells. *Prog. Neurobiol.* 17, 141–184.

Pressley, T. J. (1992). Phylogenetic conservation of isoform-specific regions within the α sub-unit of Na+-K+ ATPase. *Am. J. Physiol.* 262, C743–751.

Rowe, S. J., Messenger, N. J., and Warner, A. E. (1993). The role of noradrenaline in the differentiation of amphibian embryonic neurones. *Development* 119, 1343–1357.

Sambrook, J., Fritsch, E. F., and Maniatis, T. (1989). ''Molecular Cloning: A Laboratory Manual,'' 2nd ed., Cold Spring Harbor Laboratory Press, Cold Spring Harbor, NY.

Sanger, F., Nicklen, S., and Coulson, A. R. (1977). DNA sequencing with chain-terminating inhibitors. *Proc. Natl. Acad. Sci. USA* 74, 5463.

Shull, G. E., Schwartz, A., and Lingrel, J. B. (1985). Amino acid sequence of the catalytic subunit of the (Na^+ + K^+) ATPase deduced from a complementary cDNA. *Nature London* 316, 691–695.

Slack, C., and Warner, A. E. (1973). Intracellular and intercellular potentials in the early amphibian embryo. *J. Physiol.* 232, 313–330.

Slack, C., Warner, A. E., and Warren, R. L. (1973). The distribution of sodium and potassium in the amphibian embryo during early development. *J. Physiol.* 232, 297–312.

Verrey, F., Kairouz, P., Schaerer, E., Fuentes, P., Geering, K., Rossier, B. C., and Kraehenbuhl, J. P. (1989). Primary sequence of *Xenopus laevis* Na^+-K^+-ATPase and its localization in A6 kidney cells. *Am. J. Physiol.* 256, F1034–1043.

Zimmerman, K., Shih, J., Bars, J., Collazo, A., and Anderson, D. J. (1993). XASH-3, a novel *Xenopus achaete-scute* homolog, provides an early marker of planar neural induction and position along the mediolateral axis of the neural plate. *Development* 119, 221–232.

Received for publication October 3, 1995
Accepted January 29, 1996